Reconstructing quintom from WMAP 5-year observations: Generalized ghost condensate

Jingfei Zhang[1] and Yuan-Xing Gui[2]

[1]*Department of Physics, College of Sciences, Northeastern University, Shenyang 110004, China*
[2]*School of Physics and Optoelectronic Technology, Dalian University of Technology, Dalian 116024, China*

In the 5-year WMAP data analysis, a new parametrization form for dark energy equation-of-state was used, and it has been shown that the equation-of-state, $w(z)$, crosses the cosmological-constant boundary $w = -1$. Based on this observation, in this paper, we investigate the reconstruction of quintom dark energy model. As a single-real-scalar-field model of dark energy, the generalized ghost condensate model provides us with a successful mechanism for realizing the quintom-like behavior. Therefore, we reconstruct this scalar-field quintom dark energy model from the WMAP 5-year observational results. As a comparison, we also discuss the quintom reconstruction based on other specific dark energy ansatzs, such as the CPL parametrization and the holographic dark energy scenarios.

I. INTRODUCTION

Observations of high-redshift supernovae indicate that the universe is accelerating at the present stage [1] and this accelerating expansion also has been confirmed by many other cosmological experiments, such as observations of large scale structure (LSS) [2], and measurements of the cosmic microwave background (CMB) anisotropy [3]. We refer to the cause for this cosmic acceleration as "dark energy," which is a mysterious exotic matter with large enough negative pressure and whose energy density has been a dominative power of the universe. The combined analysis of cosmological observations suggests that the universe is consists of about 70% dark energy, 30% dust matter (cold dark matter plus baryons), and negligible radiation. The astrophysical feature of dark energy is that it remains unclustered at all scales where gravitational clustering of baryons and nonbaryonic cold dark matter can be seen. Its gravity effect is shown as a repulsive force so as to make the expansion of the universe accelerate when its energy density becomes dominative power of the universe.

Although the nature and origin of dark energy are unknown, we still can propose some candidates to describe the properties of dark energy. The most obvious theoretical candidate of dark energy is the cosmological constant Λ (vacuum energy) [4] with an equation of state $w = -1$. The cosmological constant is rather popular in researches of cosmology and astrophysics due to its theoretical simpleness and its great success in fitting with observational data. However, as is well known, the two fundamental problems, namely the "fine-tuning" problem and the "cosmic coincidence" problem [5], still puzzle us. Theorists have made many efforts to try to resolve the cosmological constant problem, but all of these efforts turn out to be unsuccessful [6].

Also, there are other alternatives to the cosmological constant. An alternative proposal to explaining dark energy is the dynamical dark energy scenario. The dynamical dark energy proposal is often realized by some scalar field mechanism which suggests that the energy form with negative pressure is provided by a scalar field slowly rolling down its potential. So far, a lot of scalar-field dark energy models have been studied. The models such as quintessence [7], K-essence [8], phantom [9], tachyon [10] and ghost condensate [11, 12] are all famous examples of scalar-field dark energy models. In these models, the quintessence with a canonical kinetic term evolves its equation of state in the region of $w \geqslant -1$ whereas the model of phantom with negative kinetic term can always lead to $w \leqslant -1$; the K-essence can realize both $w > -1$ and $w < -1$, but it has been shown that it is very difficult for K-essence to achieve w of crossing -1 [13].

However, the analysis of the current observational data shows that the equation of state of dark energy w is likely to cross the cosmological-constant boundary (or phantom divide) -1, i.e. w is larger than -1 in the recent past and less than -1 today. The dynamical evolving behavior of dark energy with w getting across -1 has brought forward great challenge to the model-building of scalar-field in the cosmology. Just as mentioned above, the scalar-field models, such as quintessence, K-essence, phantom, cannot realize the transition of w from $w > -1$ to $w < -1$ or vice versa. Hence, the quintom model was proposed for describing the dynamical evolving behavior of w crossing -1 [14] with double fields of quintessence and phantom. The cosmological evolution of such model has been investigated in detail [15, 16]. For the single real scalar field models, the transition of crossing -1 for w can occur for the Lagrangian density $p(\phi, X)$, where X is a kinematic term of a scalar-field ϕ, in which $\partial p/\partial X$ changes sign from positive to negative, thus we require nonlinear terms in X to realize the $w = -1$ crossing [12, 13, 17]. When adding a high derivative term to the kinetic term X in the single scalar field model, the energy-momentum tensor is proven to be equivalent to that of a two-field quintom model [18]. It is remarkable that the generalized ghost condensate model of a single real scalar field is a successful realization of the quintom-like dark energy [19, 20]. What's more, a generalized ghost condensate model was investigated in Refs. [19, 20] by means of the cosmological reconstruction program. For another interesting single-field quintom model see Ref. [21], where the $w = -1$ crossing is implemented with the help of a fixed background vector field. Besides, there are also many other interesting models, such as holographic dark energy model [22] and braneworld model [23], being able to realize the quintom-like behavior.

In any case, these dark energy models including the dy-

namical dark energy models have to face the test of cosmological observations. A typical approach for this is to predict the cosmological evolution behavior of the models, by putting in the Lagrangian (in particular the potential) by hand or theoretically, and to make a consistency check of models by comparing it with observations. An alternative approach is to reconstruct corresponding theoretical Lagrangian, by using the observational data. The reconstruction of scalar-field dark energy models has been widely studied. For a minimally coupled scalar field with a potential $V(\phi)$, the reconstruction is simple and straightforward [24]. Saini et al. [25] reconstructed the potential and the equation of state of the quintessence field by parameterizing the Hubble parameter $H(z)$ based on a versatile analytical form of the luminosity distance $d_L(z)$. This method can be generalized to a variety of models, such as scalar-tensor theories [26], $f(R)$ gravity [27], K-essence model [28, 29], and also tachyon model [30], etc.. Tsujikawa has investigated the reconstruction of general scalar-field dark energy models in detail [19].

In this paper, we will investigate the quintom reconstruction from the Wilkinson Microwave Anisotropy Probe (WMAP) 5-year observations. We will focus on the generalized ghost condensate model and will reconstruct this quintom scalar-field model using various dark energy ansatzs including the parametric forms of dark energy and holographic dark energy scenarios. In particular, we will put emphasis on a new parametrization form proposed by WMAP team in Ref. [31].

The paper is organized as follows: In section II we address the dark energy parametrization proposed in Ref. [31] and describe the corresponding analysis results of the WMAP5 observations. In section III we perform a cosmological reconstruction for the generalized ghost condensate model from various dark energy ansatzs and the fitting results of the up-to-date observational data. Finally we give the concluding remarks in section IV.

II. A NEW DARK ENERGY PARAMETRIZATION IN WMAP5

The distinctive feature of the cosmological constant or vacuum energy is that its equation of state is always exactly equal to -1. Whereas, the dynamical dark energy exhibits a dynamic feature that its equation-of-state as well as its energy density are evolutionary with time. An efficient approach to probing the dynamics of dark energy is to parameterize dark energy and then to determine the parameters using various observational data. One can explore the dynamical evolution behavior of dark energy efficiently by making use of this way, although the results obtained are dependent on the parametrizations of dark energy more or less.

Among the various parametric forms of dark energy, the minimum complexity required to detect time variation in dark energy is to add a second parameter to measure a change in the equation-of-state parameter with redshift. This is the so-called linear expansion parametrization $w(z) = w_0 + w'z$, where $w' \equiv dw/dz|_{z=0}$, which was first used by Di Pietro & Claeskens [32] and later by Riess et al. [33]. However, when

some "longer-armed" observations, e.g. CMB and LSS data, are taken into account, this form of $w(z)$ will be unsuitable due to the divergence at high redshift. The most commonly used form of equation-of-state, $w(z) = w_0 + w_a z/(1 + z)$, suggested by Chevallier & Polarski [34] and Linder [35] (hence, hereafter, this form is called CPL parametrization, for convenience), can avoid the divergence problem effectively. It should be noted that this parametrization form has been investigated enormously in exploring the dynamical property of dark energy in light of observational data. However, this form cannot be adopted as it is when one uses the CMB data to constrain $w(a)$ [31]. Since this form is basically the leading-order term of a Taylor series expansion, the value of $w(a)$ can become unreasonably too large or too small when extrapolated to the decoupling epoch at $z_* \simeq 1090$ (or $a_* \simeq 9.17 \times 10^{-4}$), and thus one cannot extract meaningful constraints on the quantities such as w_0 and w_a that are defined at the *present epoch*.

In order to avoid this problem, a new parametrized form was proposed by the WMAP team [31],

$$w(a) = \frac{a\tilde{w}(a)}{a + a_{\text{trans}}} - \frac{a_{\text{trans}}}{a + a_{\text{trans}}}, \tag{1}$$

(here, it is marked as "WMAP5 parametrization") where

$$\tilde{w}(a) = \tilde{w}_0 + (1 - a)\tilde{w}_a, \tag{2}$$

and $a_{\text{trans}} = 1/(1 + z_{\text{trans}})$ is the "transition epoch," and z_{trans} is the transition redshift. In this form, $w(a)$ approaches to -1 at early times and the dark energy density tends to a constant value at $a < a_{\text{trans}}$. The dark energy density remains totally sub-dominant relative to the matter density at the decoupling epoch. At late times, $a > a_{\text{trans}}$, one recovers the widely used CPL form [35], $w(a) = w_0 + (1 - a)w_a$.

In "WMAP5 parametrization", the present-day value of w, $w_0 \equiv w(z = 0)$, and the first derivative, $w' \equiv dw/dz|_{z=0}$, are chosen as the free parameters, in stead of the $\tilde{w}_0$ and $\tilde{w}_a$.

In Ref. [31], the WMAP group constrains w_0 and w' in a flat universe from the WMAP distance priors (l_A, R, z_*), combined with the Baryon Acoustic Oscillations (BAO) and the Type Ia supernovae (SN) data. The results are that, for $z_{\text{trans}} = 10$, the 95% limit on w_0 is $-0.33 < 1 + w_0 < 0.21$; the 68% intervals are $w_0 = -1.06 \pm 0.14$ and $w' = 0.36 \pm 0.62$. Note that Ref. [36] shows that the two-dimensional distribution extends more towards south-east, i.e., $w > -1$ and $w' < 0$, when the spatial curvature is allowed. The evolutionary behavior of $w(z)$ is plotted in Fig. 1, using the best-fit results. It should be noted that that Fig. 1 is slightly different from Fig. C1 of Ref. [31] in that the revised best-fit values, $w_0 = -1.06$ and $w' = 0.36$, are used in plotting this figure.

In this section, we have briefly introduced the new parametrization of dark energy equation-of-state proposed by the WMAP team in the 5-year observations. The advantage of this parameterized form is that the value of $w(a)$ is still reasonable when extrapolated to the early times such as the decoupling epoch. We shall use this parametrization with the observational constraint result to reconstruct the generalized ghost condensate model in the next section. As a comparison, we will also discuss other specific cases, such as the CPL
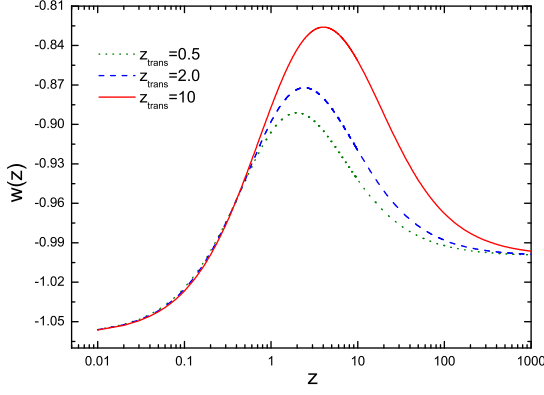
FIG. 1: The evolution of the equation of state of dark energy, corresponding to the WMAP5 parametrization with $w_0 = -1.06$ and $w' = 0.36$, for the transition redshift $z_{\text{trans}} = 0.5$, 2.0 and 10, respectively.

parametrization as well as the holographic dark energy scenarios. This work is different from the previous ones [19, 20] in that the reconstruction is implemented up to the decoupling epoch at $z_* \simeq 1090$.

III. GENERALIZED GHOST CONDENSATE MODEL AND ITS RECONSTRUCTION

As mentioned above, the dynamical dark energy can be realized by some scalar-field mechanism. In particular, the quintom model was proposed for describing the dynamical evolving behavior of w crossing -1. The results of the current observational data analysis show that the equation of sate of dark energy is likely to cross -1, see, for example, Fig. 1. So, it is necessary to realize such a quintom behavior using some scalar field mechanism. It is remarkable that the generalized ghost condensate model is a successful single-real-scalar-field quintom model. In this section, we shall focuss on the reconstruction of the generalized ghost condensate model from the WMAP 5-year observations. We will first briefly review the generalized ghost condensate model of dark energy. Then, we will implement the scalar-field dark energy reconstruction according to the WMAP5 parametrization. As a comparison, we will also perform the same reconstruction program for other specific models such as the CPL parametrization and the holographic dark energy scenarios.

A. Generalized ghost condensate model

First, let us consider the Lagrangian density of a general scalar field $p(\phi, X)$, where $X = -g^{\mu\nu}\partial_\mu\phi\partial_\nu\phi/2$ is the kinetic energy term. Note that $p(\phi, X)$ is a general function of ϕ and X, and we have used a sign notation $(-, +, +, +)$. Identifying the energy momentum tensor of the scalar field with that of a perfect fluid, we can easily derive the energy density of dark energy, $\rho_{\text{de}} = 2Xp_X - p$, where $p_X = \partial p/\partial X$. Thus, in

a spatially flat Friedmann-Robertson-Walker (FRW) universe involving dust matter (baryon plus dark matter) and dark energy, the dynamic equations for the scalar field are

$$3H^2 = \rho_{\text{m}} + 2Xp_X - p, \tag{3}$$

$$2\dot{H} = -\rho_{\text{m}} - 2Xp_X, \tag{4}$$

where $X = \dot{\phi}^2/2$ in the cosmological context, and note that we have used the unit $M_P = 1$ for convenience. Introducing a dimensionless quantity

$$r \equiv E^2 = H^2/H_0^2, \tag{5}$$

we find from Eqs. (3) and (4) that

$$p = [(1 + z)r' - 3r]H_0^2, \tag{6}$$

$$\phi'^2 p_X = \frac{r' - 3\Omega_{\text{m0}}(1 + z)^2}{r(1 + z)}, \tag{7}$$

where prime denotes a derivative with respect to z. The equation of state for dark energy is given by

$$w = \frac{p}{\phi^2 p_X - p} = \frac{(1 + z)r' - 3r}{3r - 3\Omega_{\text{m0}}(1 + z)^3}. \tag{8}$$

Next, let us consider the generalized ghost condensate model proposed in Ref. [19] (see also Ref. [20]), in which the behavior of crossing the cosmological-constant boundary can be realized, with the Lagrangian density

$$p = -X + h(\phi)X^2, \tag{9}$$

where $h(\phi)$ is a function in terms of ϕ. Actually, the function $h(\phi)$ can be explicitly expressed for the specific cases. For example, in the dilatonic ghost case, we have $h(\phi) = ce^{\lambda\phi}$ [12]. From Eqs. (6) and (7) we obtain

$$\phi'^2 = \frac{12r - 3(1 + z)r' - 3\Omega_{\text{m0}}(1 + z)^3}{r(1 + z)^2}, \tag{10}$$

$$h(\phi) = \frac{6(2(1 + z)r' - 6r + r(1 + z)^2\phi'^2)}{r^2(1 + z)^4\phi'^4}\rho_{\text{c0}}^{-1}, \tag{11}$$

$$X = \frac{1}{2}\dot{\phi}^2 = \frac{1}{6}r\phi'^2(1 + z)^2\rho_{\text{c0}}, \tag{12}$$

where $\rho_{\text{c0}} = 3H_0^2$ represents the present critical density of the universe. The crossing of the cosmological-constant boundary corresponds to $hX = 1/2$. The system can enter the phantom region ($hX < 1/2$) without discontinuous behavior of h and X.

The evolution of the field ϕ can be derived by integrating ϕ' according to Eq.(10). Note that the field ϕ is determined up to an additive constant ϕ_0, but it is convenient to take ϕ to be zero at the present epoch ($z = 0$). The function $h(\phi)$ can be reconstructed using Eq. (11) when the information of $r(z)$ is obtained from the observational data.

Generically, the Friedmann equation can be expressed as

$$r(z) = \Omega_{\text{m0}}(1 + z)^3 + (1 - \Omega_{\text{m0}})f(z), \tag{13}$$

where $f(z)$ is some function encoding the information about the dynamical property of dark energy,

$$f(z) = \exp\left[3\int_0^z \frac{1 + w(s)}{1 + s}ds\right]. \tag{14}$$

B. Reconstruction

In this subsection, we will reconstruct the function $h(\phi)$ for the ghost condensate model using some ansatzs for the equation-of-state of dark energy. We will first use the WMAP5 parametrization discussed in section II. This case is important in this paper because the ansatz is new. Next, for comparing the new ansatz with the previous ones, we will preform the same reconstruction program for other scenarios. This includes the CPL parametrization and the holographic dark energy scenarios. The reconstruction will correspond to the fitting results from the latest observational data. What's more, the reconstruction program will be implemented up to the decoupling epoch at $z_* \simeq 1090$, which is different from the previous works [19, 20] that focus only on the late times.

1. WMAP5 parametrization

First, we use the new ansatz (1) to implement the reconstruction. The reconstruction for $h(\phi)$ is plotted in Fig. 2 with transition redshift $z_{\rm trans} = 0.5$, 2 and 10, by using the best-fit results, $w_0 = -1.06$, $w' = 0.36$ and $\Omega_{\rm m0} = 0.273$, from the combined analysis of WMAP5+SN+BAO. In addition, the evolutions of the scalar field $\phi(z)$ as well as the functions $h(z)$ and $X(z)$ are also determined by the reconstruction program, see Figs. 3, 4 and 5.

From Fig. 2, we see that the reconstructed $h(\phi)$, up to $z_* \simeq 1090$, is not a monotonous function. In the rough range of z between 0 and 1, the function $h(\phi)$ is increasing, see also Fig. 4. The shape of $h(\phi)$ in this range indeed mimic an exponential function that is the case of the dilatonic ghost condensate [12]. However, in the range of z greater than 1, $h(\phi)$ is a decreasing function. Figure 5 shows the case of the kinematic energy density $X(z)$. From this figure, we find that $z \simeq 1$ is indeed a pivot point. In the range of z larger than 1, the field ϕ moves more and more slowly; in the range of z less than 1, the field ϕ moves faster and faster, albeit the change of X in this stage is slight. From Fig. 3, we can explicitly see the change rate of the field ϕ. We find that in the range of $z \sim 0.1 - 10$, the change rate of ϕ, namely $d\phi/dz$, is large; elsewhere, it is small.

One of the aims of this paper is to explore the dynamical evolution behavior of the scalar field at early times (high redshifts), by reconstructing the dynamics of the scalar field according to the observations. Previous works only focus on the low redshift evolution ($z < 2$ or so) [19, 20]. From Figs. 4 and 5, we see that at low redshifts, the cases with different $z_{\rm trans}$ behave in accordance, but at high redshifts, the difference turns on. The bigger $z_{\rm trans}$ is, the smaller h and bigger X are, at high redshifts. For the scalar field evolution, we see from Fig. 3 that the difference in the shapes of $\phi(z)$ is not big. However, the difference in shapes of $h(\phi)$ is rather evident for different $z_{\rm trans}$. Therefore, our investigation of the reconstruction explicitly exhibits the early-time dynamical evolution of the generalized ghost condensate model. We show that, for the WMAP5 parametrization, different $z_{\rm trans}$ will bring little impact at low redshifts but bring great impact at high redshifts,
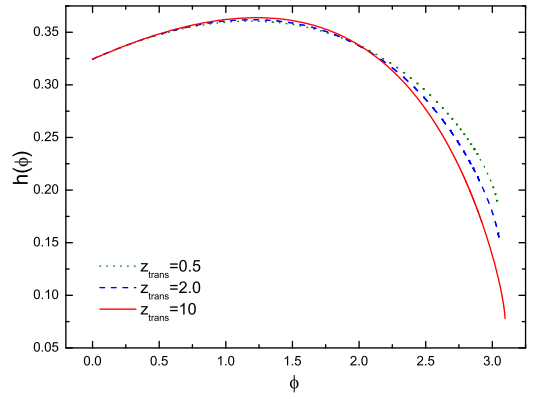

FIG. 2: Reconstruction of the generalized ghost condensate model according to the WMAP5 parametrization with the best fit results derived from WMAP5 combined with SN and BAO, $w_0 = -1.06$, $w' = 0.36$ and $\Omega_{\rm m0} = 0.273$. In this plot, we show the cases of the function $h(\phi)$, in unit of $\rho_{\rm c0}^{-1}$. The selected lines correspond to the transition redshift $z_{\rm trans} = 0.5$, 2.0 and 10, respectively.

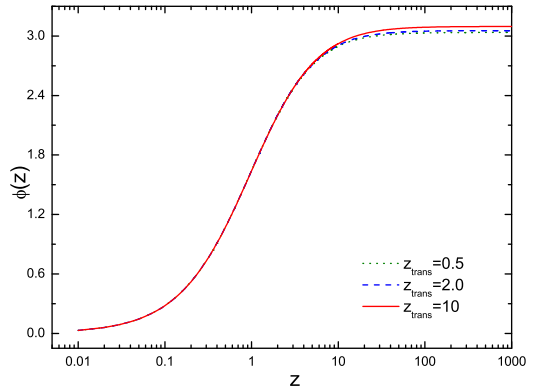
FIG. 3: Reconstruction of the generalized ghost condensate model according to the WMAP5 parametrization with transition redshift $z_{\rm trans} = 0.5$, 2.0 and 10. In this plot, we show the evolutions of the scalar field $\phi(z)$, in unit of the Planck mass M_P, corresponding to the best fit results of the joint analysis of WMAP5 + SN + BAO.

to the dynamics of scalar field.

For a comparison, we shall also investigate other cases based on different ansatzs or scenarios in what follows. In those cases, we will only show the reconstructed $h(\phi)$ and $\phi(z)$, for briefness.

2. CPL parametrization

We now consider the CPL ansatz for the equation-of-state of dark energy, $w(a) = w_0 + (1 - a)w_a$. It should be pointed out that if one extends it to an arbitrarily high redshift, it will result in an undesirable situation in which the dark energy is as important as the radiation density at the epoch of the Big Bang Nucleosynthesis (BBN). Hence, in order to constrain such a scenario, one may use the limit on the expansion rate
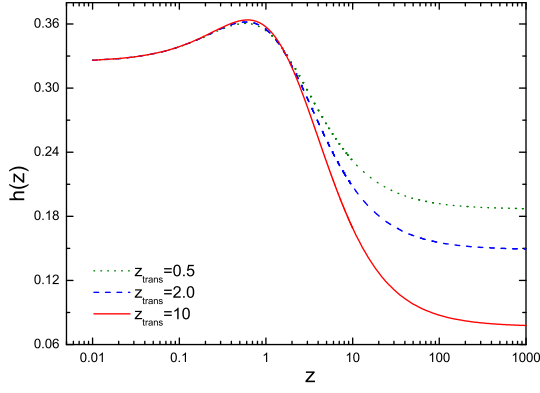
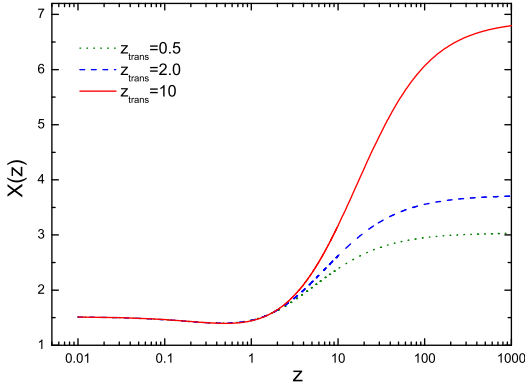FIG. 4: Reconstruction of the generalized ghost condensate model according to the WMAP5 parametrization with transition redshift z_{trans} = 0.5, 2.0 and 10. In this plot, we show the evolution of the function $h(z)$. Here h is in unit of ρ_{c0}^{-1}.
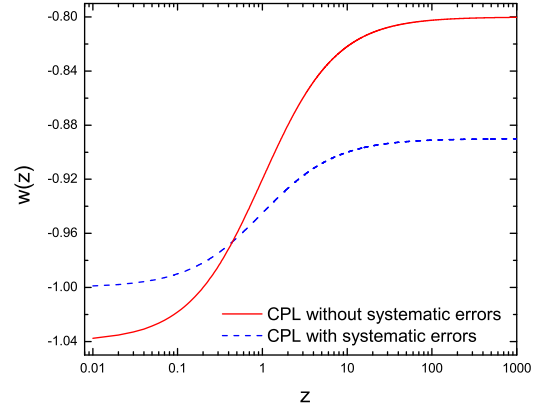

FIG. 6: The equation-of-state $w(z)$ in the CPL parametrization. In this plot, we show the two best-fit cases from WMAP5+SN+BAO+BBN, with and without SN systematic errors.

the equation-of-state are very different.

FIG. 5: Reconstruction of the generalized ghost condensate model according to the WMAP5 parametrization with transition redshift z_{trans} = 0.5, 2.0 and 10. In this plot, we show the evolution of the kinematic energy density $X = \dot{\phi}^2/2$. Here, X is in unit of ρ_{c0}.
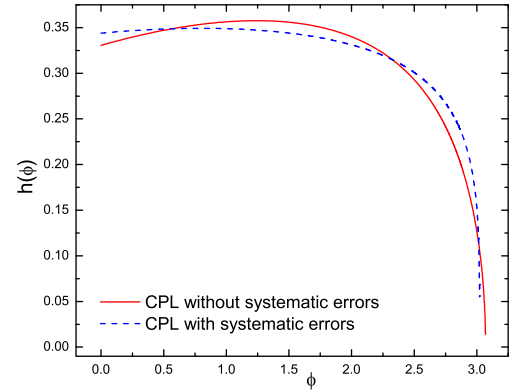

FIG. 7: Reconstruction of the generalized ghost condensate model according to the CPL parametrization with the best fit results derived from WMAP5 combined with SN, BAO, and BBN. The function $h(\phi)$ is in unit of ρ_{c0}^{-1}.

from BBN.

The WMAP team also shows in Ref. [31] the constraint on w_0 and w_a for the CPL model, $w(a) = w_0 + (1-a)w_a$, from the WMAP distance priors, the BAO and SN data, and the BBN prior in the flat universe. The 95% limit on w_0 is $-0.29 < 1 + w_0 < 0.21$ and the 68% intervals are $w_0 = -1.04 \pm 0.13$ and $w_a = 0.24 \pm 0.55$. Besides, the effects of the systematic errors are also studied. They find that $w_0 = -1.00 \pm 0.19$ and $w_a = 0.11 \pm 0.70$ with the systematic errors included.

The dark energy equation-of-state of the two cases with and without the SN systematic errors, for the CPL parametrization, at the best-fits, is plotted in Fig. 6. From this figure, one can see that when considering the SN systematic errors, the fitting results will be influenced significantly. One can find that the equation-of-state even does not cross -1 in the CPL case with the systematic errors, at the best-fit. Furthermore, comparing with the WMAP5 parametrization (see Fig. 1), it is easy to see that the early-time evolutionary behaviors for

Performing the reconstruction program, we derive the function forms of $h(\phi)$ and $\phi(z)$, shown in Figs. 7 and 8, respectively. We find that the global trend of the functions $h(\phi)$ and $\phi(z)$ of the CPL case is similar to that of the WMAP5 case (see also Figs. 2 and 3). For the function $h(\phi)$, comparing with the WMAP5 case, the late-time behaviors are very similar but the early-time behaviors are slightly different. Also, we find from Fig. 7 that the function $h(\phi)$ will be monotonously decreasing if the equation-of-state does not cross -1 (see the dashed lines in Figs. 6 and 7). For the dynamical evolution of the field ϕ, comparing Fig. 8 with Fig. 3, we find that the difference is fairly little.
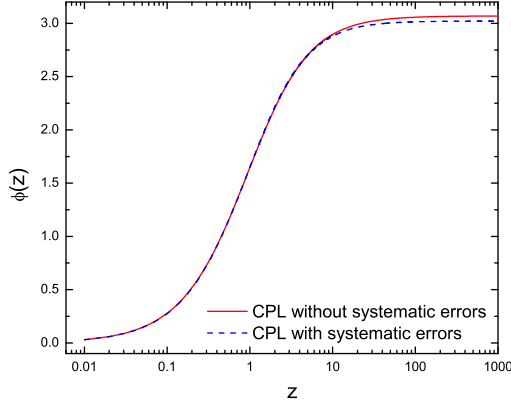
FIG. 8: Reconstruction of the generalized ghost condensate model according to the CPL parametrization with the best fit results derived from WMAP5 combined with SN, BAO, and BBN. The scalar field $\phi(z)$ is in unit of M_P.

3. Holographic dark energy scenarios

Furthermore, we also consider the holographic dark energy scenarios. The reason of considering the holographic dark energy is that we should not only consider the simple parametrizations of dark energy, but also consider some sophisticated dark energy models motivated by quantum gravity.

The holographic dark energy density can be expressed as

$$\rho_{\mathrm{de}} = 3c^2 M_P^2 L^{-2}, \tag{15}$$

where c is a numerical parameter determined by observations, and L is the infrared (IR) cutoff of the theory. Here, we explicitly write out the reduced Planck mass M_P. In the holographic dark energy models, the key problem is how to choose an appropriate IR cutoff for the theory. In the original holographic dark energy scenario proposed by Li [22], the IR cutoff is chosen as the event horizon of the universe, $R_{\mathrm{eh}} = a \int_t^\infty dt/a$. In a generalized version [29], the IR cutoff is taken as the average of the Ricci scalar curvature, $|\mathcal{R}|^{-1/2}$. This new version is often called "Ricci dark energy." It should be mentioned that the two scenarios of holographic dark energy both exhibit quintom feature [22, 29, 37].

Recently, the holographic dark energy models were constrained by the latest observational data, WMAP5+BAO+SN, see Ref. [38]. For the holographic dark energy, we have the fitting results: For 68.3% confidence level, $\Omega_{\mathrm{m0}} = 0.277^{+0.022}_{-0.021}$, and $c = 0.818^{+0.113}_{-0.097}$; for 95.4% confidence level, $\Omega_{\mathrm{m0}} = 0.277^{+0.037}_{-0.034}$, and $c = 0.818^{+0.196}_{-0.154}$. For the Ricci dark energy, we have the fitting results: For 68.3% confidence level, $\Omega_{\mathrm{m0}} = 0.324^{+0.024}_{-0.022}$, and $c^2 = 0.371^{+0.023}_{-0.023}$; for 95.4% confidence level, $\Omega_{\mathrm{m0}} = 0.324^{+0.040}_{-0.036}$, and $c^2 = 0.371^{+0.037}_{-0.038}$. The dark-energy equation of state, at the best fits, in these two scenarios is shown in Fig. 9. One can see from this figure that although both originated from the holographic principle of quantum gravity, different IR cutoffs will bring so different cosmological consequences. We shall make use of the best-fit

results to reconstruct the ghost condensate model in the following.
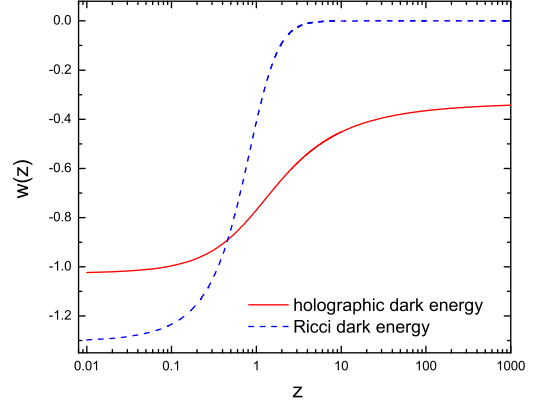

FIG. 9: The equation-of-state $w(z)$ in the holographic dark energy scenarios. In this plot, we show the best-fit cases from WMAP5+SN+BAO.

The reconstructed function forms of $h(\phi)$ and $\phi(z)$ are shown in Figs. 10 and 11. From these two figures, we see that the big difference in $w(z)$ is converted to the big differences in $h(\phi)$ and $\phi(z)$. The reconstructions of $h(\phi)$ and $\phi(z)$ indicate that the holographic dark energy is compatible with the previous dark energy parametrizations, but the Ricci dark energy is not. In Fig. 10, we find that there exist a sharp peak of h around $\phi \sim 1.5$ and a long tail of h in the range of $\phi > 3.5$, for the Ricci dark energy. From Fig. 11, we see that the dynamics of the field ϕ in the Ricci scenario is also larruping. Although in the range of $z < 1$, the evolutions of ϕ nearly go to degenerate, the big different occurs in the range of $z > 1$, especially in the stage of $z > 10$.
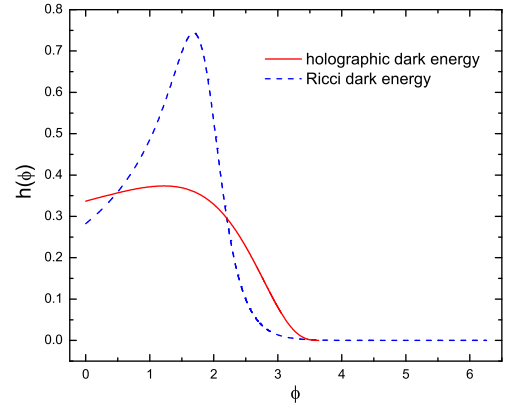

FIG. 10: Reconstruction of the generalized ghost condensate model according to the holographic dark energy scenarios with the best-fit results derived from WMAP5 combined with SN and BAO. The function $h(\phi)$ is in unit of ρ_{c0}^{-1}.

In Ref. [38], the authors use the Bayesian evidence (BE) as a model selection criterion to make a comparison between
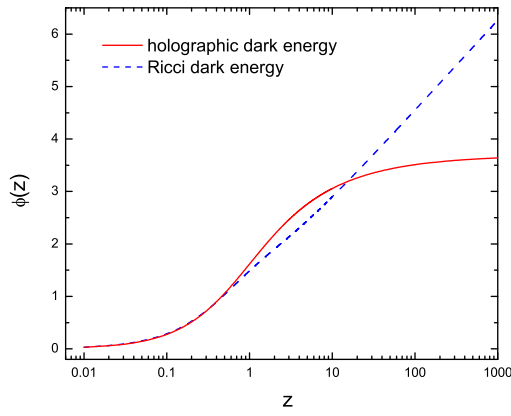
FIG. 11: Reconstruction of the generalized ghost condensate model according to the holographic dark energy scenarios with the best-fit results derived from WMAP5 combined with SN and BAO. The scalar field $\phi(z)$ is in unit of M_P.

the holographic dark energy models. It is found that for holographic dark energy and Ricci dark energy, $\Delta \ln \text{BE} = -0.86$ and -8.14, respectively. So, evidently, the holographic dark energy scenrio is more favored by the observational data, whereas the Ricci dark energy scenario looks like disfavored by the observational data. Our reconstruction investigation also supports this conclusion from another angle of view.

IV. CONCLUDING REMARKS

The recent fits to current observational data, such as SN, CMB and LSS, find that even though the behavior of dark energy is consistent to great extent with a cosmological constant, an evolving dark energy with the equation of state w larger than -1 in the recent past but less than -1 today is also with some possibility. Although the scalar-field models of dark energy, such as quintessence and phantom, can pro-

vide us with dynamical mechanism for dark energy, the behavior of cosmological-constant crossing brings forward a great challenge to the model-building for dynamical dark energy, because neither quintessence nor phantom can fulfill this behavior. A two-field quintom model, therefore, was suggested to realize this behavior by means of the incorporation of the features of quintessence and phantom. Besides, the generalized ghost condensate model provides us with a successful single-real-scalar-field model for realizing the quintom-like behavior. For probing the dynamical nature of dark energy, one should parameterize dark energy first and then constrain the parameters using the observational data.

In this paper, we have investigated the dynamical behavior of the general ghost condensate scalar-field model by taking a new form of parametrization of the equation of state proposed in Ref. [31] and the best-fit values from the observational data. The results of reconstruction show the dynamical behavior of the generalized ghost condensate from this parametrization. In particular, this reconstruction investigation explores the early-time evolutionary behavior of the scalar field model. As a comparison, we also discussed other specific cases including the CPL parametrization and the holographic dark energy scenarios.

The increase of the quantity and quality of observational data in the future will undoubtedly provide a true *model-independent* manner for exploring the properties of dark energy. We hope that the future high-precision observations (e.g. SNAP) may be capable of providing us with deep insight into the nature of dark energy driving the acceleration of the universe.

ACKNOWLEDGMENTS

[1] A. G. Riess *et al.* [Supernova Search Team Collaboration], Astron. J. **116**, 1009 (1998) [astro-ph/9805201]; S. Perlmutter *et al.* [Supernova Cosmology Project Collaboration], Astrophys. J. **517**, 565 (1999) [astro-ph/9812133].

[2] M. Tegmark *et al.* [SDSS Collaboration], Phys. Rev. D **69**, 103501 (2004) [astro-ph/0310723]; K. Abazajian *et al.* [SDSS Collaboration], Astron. J. **128**, 502 (2004) [astro-ph/0403325]; K. Abazajian *et al.* [SDSS Collaboration], Astron. J. **129**, 1755 (2005) [astro-ph/0410239].

[3] D. N. Spergel *et al.* [WMAP Collaboration], Astrophys. J. Suppl. **148**, 175 (2003) [astro-ph/0302209].

[4] A. Einstein, Sitzungsber. K. Preuss. Akad. Wiss. 142 (1917).

[5] P. J. Steinhardt, in *Critical Problems in Physics*, edited by V. L. Fitch and D. R. Marlow (Princeton University Press, Princeton, NJ, 1997).

[6] S. Weinberg, Rev. Mod. Phys. **61** 1 (1989).

[7] P. J. E. Peebles and B. Ratra, Astrophys. J. **325** L17 (1988);

B. Ratra and P. J. E. Peebles, Phys. Rev. D **37** 3406 (1988); C. Wetterich, Nucl. Phys. B **302** 668 (1988); J. A. Frieman, C. T. Hill, A. Stebbins and I. Waga, Phys. Rev. Lett. **75**, 2077 (1995) [astro-ph/9505060]; M. S. Turner and M. J. White, Phys. Rev. D **56**, 4439 (1997) [astro-ph/9701138]; A. R. Liddle and R. J. Scherrer, Phys. Rev. D **59**, 023509 (1999) [astro-ph/9809272]; I. Zlatev, L. M. Wang and P. J. Steinhardt, Phys. Rev. Lett. **82**, 896 (1999) [astro-ph/9807002]; P. J. Steinhardt, L. M. Wang and I. Zlatev, Phys. Rev. D **59**, 123504 (1999) [astro-ph/9812313]; X. Zhang, Mod. Phys. Lett. A **20**, 2575 (2005) [astro-ph/0503072]; X. Zhang, Phys. Lett. B **611**, 1 (2005) [astro-ph/0503075].

[8] C. Armendariz-Picon, V. F. Mukhanov and P. J. Steinhardt, Phys. Rev. Lett. **85**, 4438 (2000) [astro-ph/0004134]; C. Armendariz-Picon, V. F. Mukhanov and P. J. Steinhardt, Phys. Rev. D **63**, 103510 (2001) [astro-ph/0006373].

[9] R. R. Caldwell, Phys. Lett. B **545**, 23 (2002)

[astro-ph/9908168].

[10] A. Sen, JHEP **0207**, 065 (2002) [hep-th/0203265]; T. Padman-abhan, Phys. Rev. D **66**, 021301 (2002) [hep-th/0204150].

[11] N. Arkani-Hamed, H. C. Cheng, M. A. Luty and S. Muko-hyama, JHEP **0405**, 074 (2004) [hep-th/0312099]; S. Muko-hyama, JCAP **0610**, 011 (2006) [hep-th/0607181].

[12] F. Piazza and S. Tsujikawa, JCAP **0407**, 004 (2004) [hep-th/0405054].

[13] A. Vikman, Phys. Rev. D **71**, 023515 (2005) [astro-ph/0407107].

[14] B. Feng, X. L. Wang and X. M. Zhang, Phys. Lett. B **607**, 35 (2005) [astro-ph/0404224].

[15] Z. K. Guo, Y. S. Piao, X. M. Zhang and Y. Z. Zhang, Phys. Lett. B **608**, 177 (2005) [astro-ph/0410654]; X. Zhang, Com-mun. Theor. Phys. **44**, 762 (2005); X. F. Zhang, H. Li, Y. S. Piao and X. M. Zhang, Mod. Phys. Lett. A **21**, 231 (2006) [astro-ph/0501652].

[16] Y. F. Cai, H. Li, Y. S. Piao and X. M. Zhang, Phys. Lett. B **646**, 141 (2007) [arXiv:gr-qc/0609039]; Y. F. Cai, T. Qiu, Y. S. Piao, M. Li and X. M. Zhang, JHEP **0710**, 071 (2007) [arXiv:0704.1090 [gr-qc]]; H. H. Xiong, Y. F. Cai, T. Qiu, Y. S. Piao and X. M. Zhang, Phys. Lett. B **666**, 212 (2008) [arXiv:0805.0413 [astro-ph]]; R. Lazkoz, G. Leon and I. Quiros, Phys. Lett. B **649**, 103 (2007) [arXiv:astro-ph/0701353]; H. Wei and R. G. Cai, Phys. Lett. B **634**, 9 (2006) [arXiv:astro-ph/0512018]; S. G. Shi, Y. S. Piao and C. F. Qiao, JCAP **0904**, 027 (2009) [arXiv:0812.4022 [astro-ph]]; M. R. Setare and E. N. Sari-dakis, arXiv:0807.3807 [hep-th]; L. P. Chimento, M. Forte, R. Lazkoz and M. G. Richarte, Phys. Rev. D **79**, 043502 (2009) [arXiv:0811.3643 [astro-ph]].

[17] A. Anisimov, E. Babichev and A. Vikman, JCAP **0506**, 006 (2005) [astro-ph/0504560].

[18] M. Z. Li, B. Feng and X. M. Zhang, JCAP **0512**, 002 (2005) [hep-ph/0503268].

[19] S. Tsujikawa, Phys. Rev. D **72**, 083512 (2005) [astro-ph/0508542].

[20] X. Zhang, Phys. Rev. D **74**, 103505 (2006) [astro-ph/0609699]; X. Zhang, Phys. Rev. D **79**, 103509 (2009) [arXiv:0901.2262 [astro-ph.CO]]; J. Zhang, X. Zhang and H. Liu, Mod. Phys. Lett. A **23**, 139 (2008) [arXiv:astro-ph/0612642]; C. J. Feng, Phys. Lett. B **672**, 94 (2009) [arXiv:0810.2594 [hep-th]].

[21] C. G. Huang and H. Y. Guo, astro-ph/0508171.

[22] M. Li, Phys. Lett. B **603**, 1 (2004) [hep-th/0403127]; Q. G. Huang and M. Li, JCAP **0408**, 013 (2004) [astro-ph/0404229]; Q. G. Huang and Y. G. Gong, JCAP **0408**, 006 (2004) [astro-ph/0403590]; Q. G. Huang and M. Li, JCAP **0503**, 001 (2005) [hep-th/0410095]; X. Zhang, Int. J. Mod. Phys. D **14**, 1597 (2005) [astro-ph/0504586]; X. Zhang and F. Q. Wu, Phys. Rev. D **72**, 043524 (2005) [astro-ph/0506310]; Z. Chang, F. Q. Wu and X. Zhang, Phys. Lett. B **633**, 14 (2006) [astro-ph/0509531]; X. Zhang and F. Q. Wu, Phys. Rev. D **76**, 023502 (2007) [arXiv:astro-ph/0701405]; J. Zhang, X. Zhang and H. Liu, Eur. Phys. J. C **52**, 693 (2007) [arXiv:0708.3121 [hep-th]]; M. R. Setare, J. Zhang and X. Zhang, JCAP **0703**, 007 (2007) [arXiv:gr-qc/0611084]; J. Zhang, X. Zhang and H. Liu, Phys. Lett. B **659**, 26 (2008) [arXiv:0705.4145 [astro-ph]]; M. Li, X. D. Li, C. S. Lin and Y. Wang, Commun. Theor. Phys. **51**, 181 (2009) [arXiv:0811.3332 [hep-th]]; X. Zhang, arXiv:0909.4940 [gr-qc].

[23] R. G. Cai, H. S. Zhang and A. Wang, Commun. Theor. Phys. **44**, 948 (2005) [hep-th/0505186].

[24] A. A. Starobinsky, JETP Lett. **68**, 757 (1998) [astro-ph/9810431]; D. Huterer and M. S. Turner, Phys. Rev. D **60**, 081301 (1999) [astro-ph/9808133]; T. Nakamura and T. Chiba, Mon. Not. R. Astron. Soc. **306**, 696 (1999) [astro-ph/9810447]; Z. K. Guo, N. Ohta and Y. Z. Zhang, Phys. Rev. D **72**, 023504 (2005) [astro-ph/0505253]; X. Zhang, Phys. Lett. B **648**, 1 (2007) [arXiv:astro-ph/0604484]; Z. K. Guo, N. Ohta and Y. Z. Zhang, astro-ph/0603109; Y. Z. Ma and X. Zhang, Phys. Lett. B **661**, 239 (2008) [arXiv:0709.1517 [astro-ph]].

[25] T. D. Saini, S. Raychaudhury, V. Sahni and A. A. Starobinsky, Phys. Rev. Lett. **85**, 1162 (2000) [astro-ph/9910231].

[26] B. Boisseau, G. Esposito-Farese, D. Polarski and A. A. Starobinsky, Phys. Rev. Lett. **85**, 2236 (2000) [gr-qc/0001066]; G. Esposito-Farese and D. Polarski, Phys. Rev. D **63**, 063504 (2001) [gr-qc/0009034]; L. Perivolaropoulos, JCAP **0510**, 001 (2005) [astro-ph/0504582].

[27] S. Capozziello, V.F. Cardone and A. Troisi, Phys. Rev. D **71**, 043503 (2005) [astro-ph/0501426]; X. Wu and Z. H. Zhu, Phys. Lett. B **660**, 293 (2008) [arXiv:0712.3603 [astro-ph]]; C. J. Feng, arXiv:0812.2067 [hep-th].

[28] H. Li, Z. K. Guo and Y. Z. Zhang, astro-ph/0601007.

[29] C. Gao, F. Q. Wu, X. Chen and Y. G. Shen, Phys. Rev. D **79**, 043511 (2009) [arXiv:0712.1394 [astro-ph]].

[30] J. Zhang, X. Zhang and H. Liu, Phys. Lett. B **651**, 84 (2007) [arXiv:0706.1185 [astro-ph]]; J. Cui, L. Zhang, J. Zhang and X. Zhang, arXiv:0902.0716 [astro-ph.CO].

[31] E. Komatsu *et al.* [WMAP Collaboration], Astrophys. J. Suppl. **180**, 330 (2009) [arXiv:0803.0547 [astro-ph]].

[32] E. Di Pietro and J. F. Claeskens, Mon. Not. Roy. Astron. Soc. **341**, 1299 (2003) [astro-ph/0207332].

[33] A. G. Riess *et al.* [Supernova Search Team Collaboration], As-trophys. J. **607**, 665 (2004) [astro-ph/0402512].

[34] M. Chevallier and D. Polarski, Int. J. Mod. Phys. D **10**, 213 (2001) [gr-qc/0009008].

[35] E. V. Linder, Phys. Rev. Lett. **90**, 091301 (2003) [astro-ph/0208512].

[36] Y. Wang and P. Mukherjee, Phys. Rev. D **76**, 103533 (2007) [arXiv:astro-ph/0703780].

[37] C. J. Feng and X. Zhang, Phys. Lett. B **680**, 399 (2009) [arXiv:0904.0045 [gr-qc]].

[38] M. Li, X. D. Li, S. Wang and X. Zhang, JCAP **0906**, 036 (2009) [arXiv:0904.0928 [astro-ph.CO]].